RNA (1995), *1*:575–583. Cambridge University Press. Printed in the USA.

Probing RNA tertiary structure: Interhelical crosslinking of the hammerhead ribozyme

SNORRI TH. SIGURDSSON, THOMAS TUSCHL, and FRITZ ECKSTEIN

Max-Planck-Institut für experimentelle Medizin, Hermann-Rein-Str. 3, D-37075 Göttingen, Germany

ABSTRACT

Distinct structural models for the hammerhead ribozyme derived from single-crystal X-ray diffraction and fluorescence resonance energy transfer (FRET) measurements have been compared. Both models predict the same overall geometry, a wishbone shape with helices II and III nearly colinear and helix I positioned close to helix II. However, the relative orientations of helices I and II are different. To establish whether one of the models represents a kinetically active structure, a new crosslinking procedure was developed in which helices I and II of hammerhead ribozymes were disulfide-crosslinked via the 2′ positions of specific sugar residues. Crosslinking residues on helices I and II that are close according to the X-ray structure did not appreciably reduce the catalytic efficiency. In contrast, crosslinking residues closely situated according to the FRET model dramatically reduced the cleavage rate by at least three orders of magnitude. These correlations between catalytic efficiencies and spatial proximities are consistent with the X-ray structure.

Keywords: disulfide crosslinking; fluorescence resonance energy transfer; isothiocyanate; 2′-modified RNA; RNA catalysis; RNA structure; site-specific crosslinking; X-ray

INTRODUCTION

Much effort has been directed toward determining the tertiary structure of the hammerhead ribozyme and the mechanism of its site-specific RNA cleavage. Although functional group modifications of residues in the central core have identified important groups for catalysis (Bratty et al., 1993; Tuschl et al., 1993), it has not been possible to construct a three-dimensional model based on these experiments. Recently, the tertiary structure of the hammerhead ribozyme has been solved at varying levels of resolution by X-ray crystallography (Pley et al., 1994), FRET measurements (Tuschl et al., 1994), electrophoretic mobility (Bassi et al., 1995), and transient electric birefringence (Amiri & Hagerman, 1994). All of these models predict a similar wishbone shape with helices II and III nearly colinear and helix I in close proximity to helix II.

The high-resolution X-ray structure of a hammerhead ribozyme, binding a DNA substrate, explained some of the results from the functional group modifications (Pley et al., 1994), but others were not easily rationalized (Tuschl et al., 1995). Additionally, the geometry at the cleavage site did not place the required 2′-hydroxyl group in a position for an in-line attack on the phosphorus atom bearing the scissile bond. Furthermore, no metal ion, which has been postulated to participate in the cleavage reaction (Dahm & Uhlenbeck, 1991), was located close to this site. Such findings suggested that the X-ray diffraction-based structure in the crystal required a structural rearrangement in order to reach the transition state for the cleavage reaction. The question remained whether this structural rearrangement would be a local change at the cleavage site, as suggested by Pley et al. (1994), or a global change involving a reorientation of the helices.

FRET measurements on the hammerhead ribozyme, annealed to an RNA substrate containing a single deoxycytidine residue at the cleavage site, yielded the relative orientations of the three helices; this provided a starting point for the modeling of the two single-stranded central core regions (Tuschl et al., 1994). Although the FRET model and the X-ray structure both have similar global structures with respect to the placement of the helices in three-dimensional space, they differ in the relative orientation of helices I and II.

We were interested in determining whether the X-ray structure and/or the FRET model represented catalytically competent solution structures. Our approach

Reprint requests to: Fritz Eckstein, Max-Planck-Institut für experimentelle Medizin, Hermann-Rein-Str. 3, D-37075 Göttingen, Germany; e-mail: eckstein@exmed1.dnet.gwdg.de.

utilized synthetic ribozymes, each fixed in a structure resembling one of the two distinct models by the conformational constraints of an interhelix, disulfide crosslink between helices I and II. The measured catalytic activities of the crosslinked ribozymes subsequently served as an indicator for the catalytic competence of the two models.

RESULTS

Although 2′-amino groups in RNA react sluggishly with succinimidyl esters, it has been shown that they react efficiently with aromatic isothiocyanates (Aurup et al., 1994). In light of this, we undertook the synthesis of isothiocyanate **2**, which contains a protected mercaptan functionality that could subsequently be utilized to form a disulphide crosslink, after its attachment to the oligomer (Fig. 1). 3-Aminobenzyl mercaptan was prepared from 3-aminobenzyl alcohol according to the method of Frank and Smith (1946). Treatment with 2,2′-dipyridyl disulfide and acetic acid yielded the thiol-protected amine **1** (Johnson & Chenoweth, 1985), which was converted to **2** by treatment with thiophosgene in chloroform.

In order to verify that **2** reacted selectively with 2′-amino groups in RNA, the oligomers UCGCAUCGCU and UCGCA(2′-NH_2U)CGCU were incubated with **2**, under the same conditions as for the 2′-amino modified ribozymes described below. There was no measurable incorporation of **2** into the unmodified oligomer, as judged by HPLC analysis, whereas the 2′-amino modified oligomer was completely transformed (>95%) to a strongly retained product.

We prepared 2′-amino modified ribozymes 1 and 2 (Fig. 2), whose sequences were based on HH8 (Fedor & Uhlenbeck, 1992), except for residues L2.4 and 2.6, which were changed from A to U and G to C, respectively. For crosslinking, the 2′-amino groups of ribozymes 1 and 2 were reacted with **2** to yield the corresponding 2′-thiourea derivatives (Fig. 1B). After annealing the modified ribozymes to a noncleavable RNA substrate containing a deoxycytidine residue at the cleavage site, the mercaptan-protecting groups were removed by treatment with dithiothreitol (DTT). Formation of disulfide crosslinks was achieved by exposure of the thiol-containing ribozymes to oxygen in the presence of dimethylsulfoxide (DMSO). Crosslinking of both ribozymes 1 and 2 led to a major product with retarded mobility relative to the starting RNA when analyzed by 20% denaturing PAGE (DPAGE) (Fig. 3). There were also minor products formed that had strongly retarded electrophoretic mobility, presumably the products

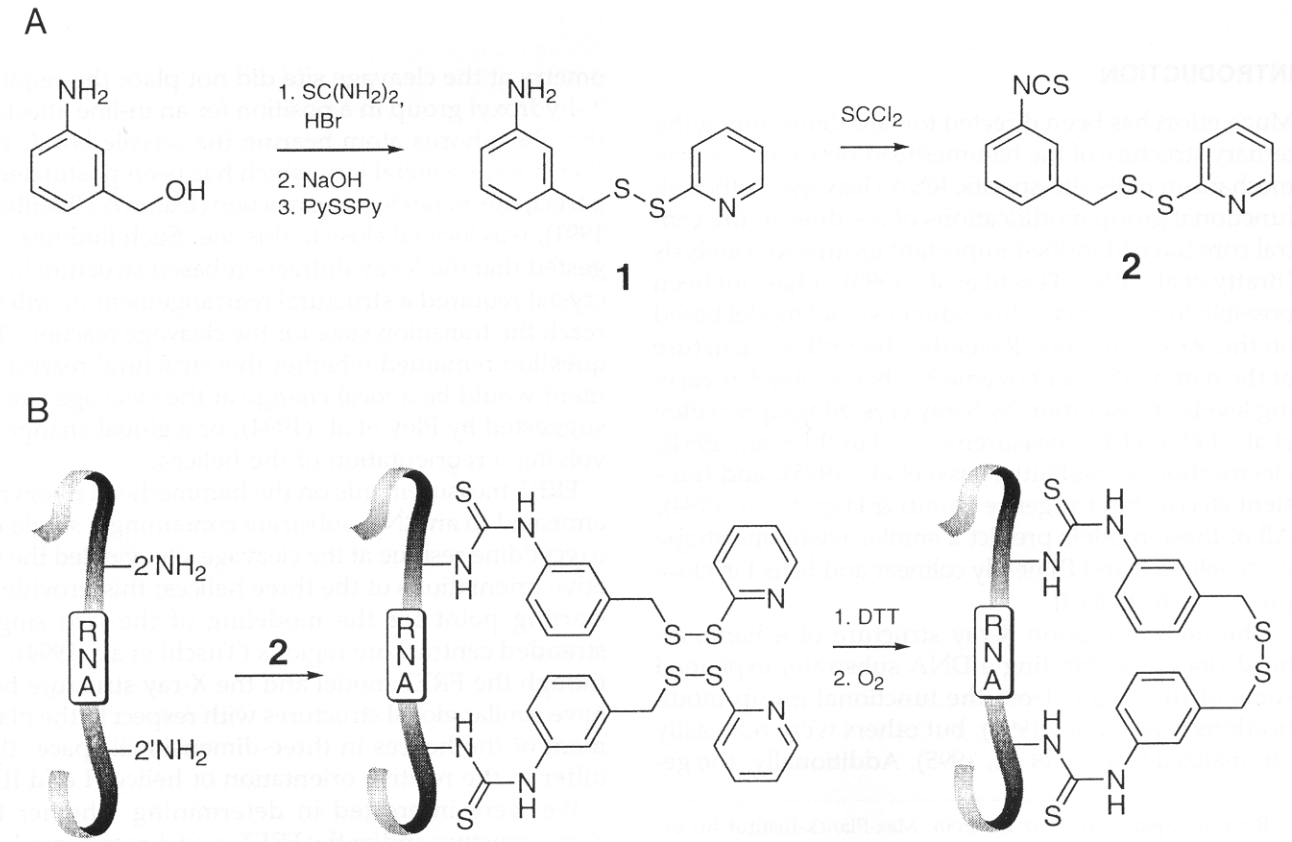

FIGURE 1. **A:** Synthesis of isothiocyanate **2**. **B:** Sequence of reactions leading to intramolecularly crosslinked ribozymes.

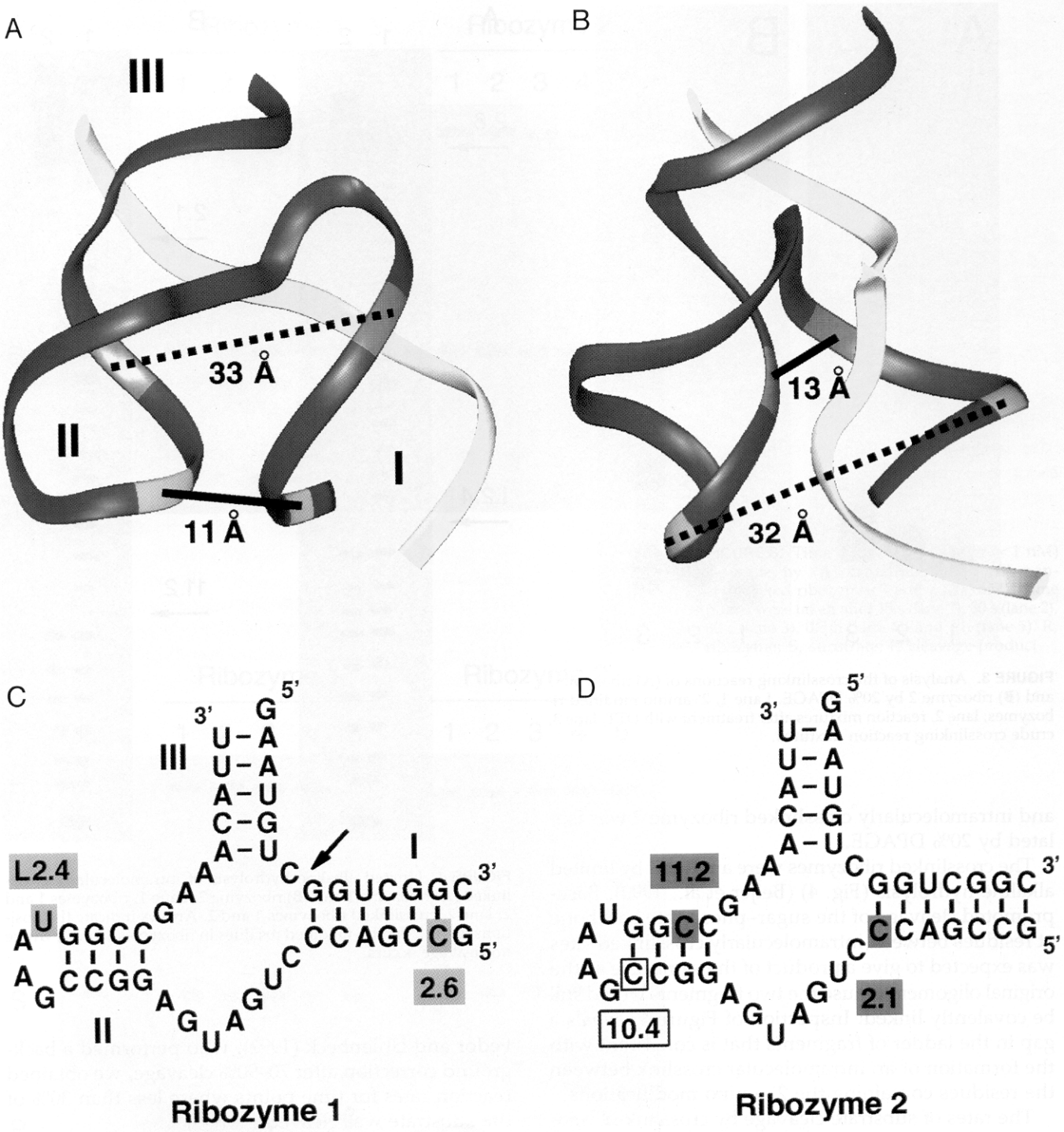

FIGURE 2. Ribbon representation of the tertiary structures of the hammerhead ribozyme based on (**A**) X-ray crystallography and (**B**) FRET solution measurements. Ribozymes and substrates are colored blue and yellow, respectively. Residues that are close in space according to the X-ray structure and the FRET model (green and red, respectively) are connected by solid lines and the broken lines represent the corresponding long distances in the other model. Distances between the 2′-hydroxyl groups of connected residues are given in Ångstroms (Å). Roman numerals indicate the number of the helices. **C,D:** RNA constructs chemically synthesized for interhelical crosslinking. Colored residues contain a 2′-amino functionality. An arrow indicates the site of cleavage. Residue 10.4, also utilized for crosslinking to test the FRET model (see text), is boxed.

from intermolecular crosslinking. The electrophoretic mobility of the major product of the crosslinking reactions, relative to that of the non-crosslinked material, varied greatly with the percentage of polyacrylamide in gels used for DPAGE. To avoid contamination by the non-crosslinked material, intramolecularly crosslinked ribozyme 1 was isolated by 12% DPAGE, where it had a higher mobility than the non-crosslinked material,

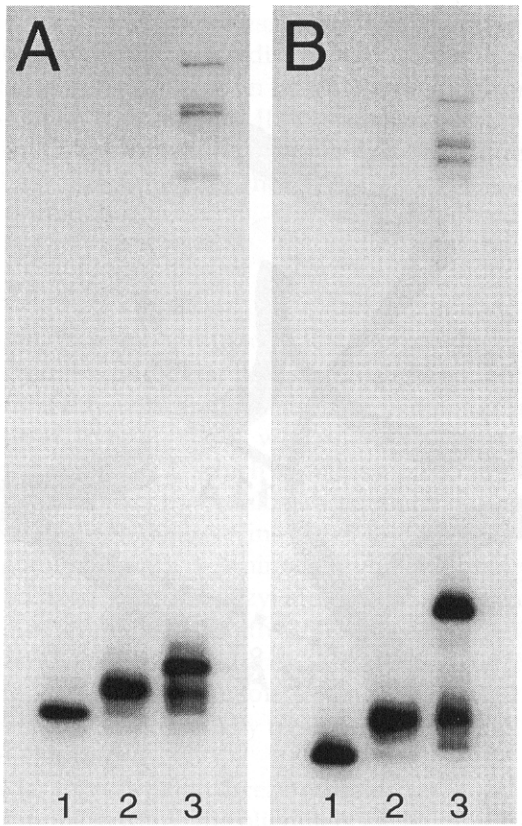

FIGURE 3. Analysis of the crosslinking reactions of (**A**) ribozyme 1 and (**B**) ribozyme 2 by 20% DPAGE. Lane 1, 2′-amino modified ribozymes; lane 2, reaction mixtures after treatment with DTT; lane 3, crude crosslinking reaction mixtures.

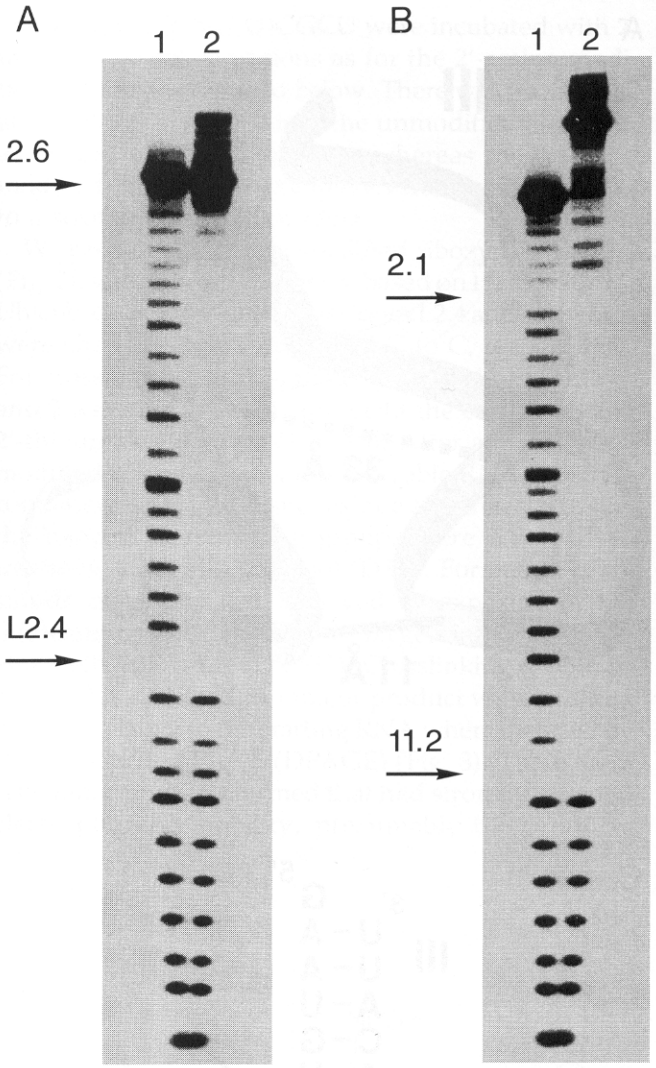

FIGURE 4. Limited alkaline hydrolysis of intramolecularly crosslinked (**A**) ribozyme 1 and (**B**) ribozyme 2. Lane 1, ribozymes 1 and 2; lane 2, crosslinked ribozymes 1 and 2. Arrows indicate the positions of the 2′-amino-modified residues in ribozymes 1 and 2, where no cleavage occurs.

and intramolecularly crosslinked ribozyme 2 was isolated by 20% DPAGE.

The crosslinked ribozymes were analyzed by limited alkaline hydrolysis (Fig. 4) (Beijer et al., 1990). Base-promoted cleavage of the sugar–phosphate backbone at residues between intramolecularly crosslinked sites was expected to give a product of the same size as the original oligomer because the two fragments would still be covalently linked. Inspection of Figure 4 reveals a gap in the ladder of fragments that is consistent with the formation of an intramolecular crosslink between the residues containing the 2′-amino modifications.

The rates of substrate cleavage by crosslinked ribozymes as well as non-crosslinked ribozymes were measured (Fig. 5; Table 1) and the single turnover kinetic parameters, k'_{cat} and K'_m, were determined as described by Fedor and Uhlenbeck (1992). The rates of cleavage, at different concentration of ribozymes (20–300 nM), were obtained by fitting the remaining fraction of uncleaved substrate, as a function of time, to a single exponential decay. The parameters k'_{cat} and K'_m were determined from Eadie–Hofstee plots. For all the ribozymes, substrate cleavage ceased when 70–85% of the substrate had been consumed; even after incubation for a few hours, substrate still remained. In contrast to Fedor and Uhlenbeck (1992), who performed a background correction after 70–90% cleavage, we obtained reaction rates for time points where less than 30% of the substrate was cleaved.

The catalytic efficiency of ribozymes 1 and 2 was similar to the reported value of 29 μM^{-1} min^{-1} for ribozyme HH8, illustrating that the 2′-amino modifications did not affect the catalytic efficiency (Fedor & Uhlenbeck, 1992). DTT reduction of crosslinked ribozymes 1 and 2 yielded the corresponding non-crosslinked ribozymes whose catalytic efficiency was within a factor of 2 from ribozymes 1 and 2, proving that introduction of the mercaptan functionality did not appreciably affect the catalytic efficiency. Crosslinked ribozyme 1 was almost as active as the corresponding non-crosslinked ribozyme, whereas the activity of ribozyme 2 was re-

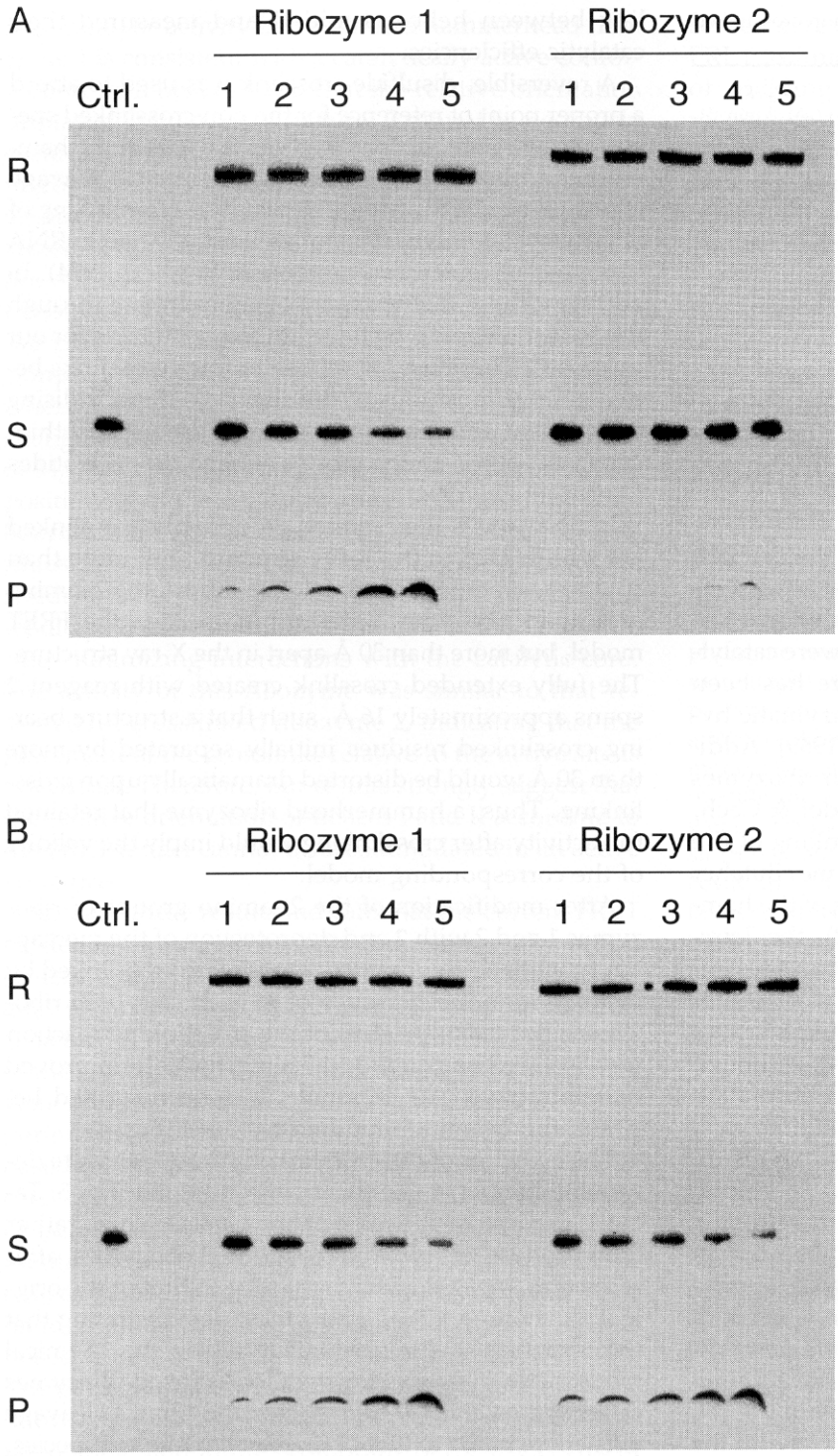

FIGURE 5. Time course of substrate (<1 nM) cleavage by (**A**) crosslinked and (**B**) non-crosslinked ribozymes 1 and 2 (200 nM). Time points were taken after 15 s (lane 1), 30 s (lane 2), 60 s (lane 3), 0.5 h (lane 4), and 2 h (lane 5). R, ribozyme; S, substrate; P, cleavage product.

duced by a factor of ca. 300 upon crosslinking. This residual activity of crosslinked ribozyme 2 was attributed to a contamination of less than 1% of non-crosslinked material.

In the event that crosslinked ribozyme 2 was inactive because of other reasons than distance constraints, we have also kinetically characterized a ribozyme that was crosslinked between residues 2.1 and 10.4. The 2′-amino groups on those residues are separated by 13 Å in the FRET model and would place the crosslink in a different position than in ribozyme 2. The results are very similar to those obtained for crosslinked ribozyme 2, namely, the observed rate constant was 0.005 min^{-1} at 500 nM ribozyme concentration and the catalytic efficiency for the non-crosslinked species was 30 μM^{-1} min^{-1}.

TABLE 1. Kinetic parameters for crosslinked and non-crosslinked ribozymes 1 and 2.[a]

Ribozyme (R)	k'_{cat} (min^{-1})	K'_m (nM)	k'_{cat}/K'_m ($\mu M^{-1}\ min^{-1}$)
R 1	0.72	19	37
R 1 XL	0.60	35	17
R 1 non-XL	0.58	25	23
R 2	0.49	20	24
R 2 XL	0.002[b]	nd	nd
R 2 non-XL	0.67	46	15

[a] XL, crosslinked; nd, not determined.
[b] Observed rate constant at 200 nM ribozyme.

DISCUSSION

The goal of this study was to determine if the detailed three-dimensional models of the hammerhead ribozyme, one based on X-ray crystallography and the other derived from FRET measurements, were catalytically competent. RNA tertiary structure has been probed using methods such as partial enzymatic hydrolysis and alkylation (Krol & Carbon, 1989). Additional methods that have been applied to ribozymes include hydroxyl radical cleavage (Celander & Cech, 1991; Wang & Cech, 1992); photo-crosslinking of the UV-sensitive element of the hairpin ribozyme (Butcher & Burke, 1994); photo-affinity crosslinking of the hammerhead ribozyme (Woisard et al., 1992), the *Tetrahymena* ribozyme (Wang et al., 1993), and ribonuclease P (Nolan et al., 1993) after incorporation of a photoactivatable group; as well as fusion of helices in the *Tetrahymena* ribozyme (Murphy et al., 1994). Although some of these methods might give more information on the tertiary structure of the hammerhead ribozyme, it is hard to envision that they could be used to distinguish between the two structural models. Therefore, we have developed a new methodology for probing the tertiary structure of RNA that was subsequently used to determine which one of the two ground-state models bears a closer resemblance to the transition-state structure.

In spite of the fact that the two models have a similar global shape, they differ fundamentally in the relative orientation of helix I and II. Qualitatively, in the X-ray structure, the minor grooves of helices I and II face each other as opposed to the major grooves that face each other at the same point of reference in the FRET model. If the hammerhead ribozyme could be independently fixed in the two structures by some means, then measurements of their catalytic efficiencies would indicate if these ground-state structures were similar to the transition-state structure of the cleavage reaction. In an attempt to accomplish this task, we have conformationally constrained two ribozyme constructs by the formation of a covalent crosslink between helices I and II and measured their catalytic efficiencies.

A reversible, disulfide crosslink was used to afford a proper point of reference for the non-crosslinked species because substitutions in sugar residues of the hammerhead ribozyme often reduce the rate of cleavage (Bratty et al., 1993). Although disulfide crosslinking of DNA is well known, it is not well established in RNA (for a recent review, see Ferentz & Verdine, 1994). In addition, these methods rely on crosslinking through the base moieties, which we judged unsuitable for our purposes. Therefore, we chose to form crosslinks between the 2′ positions of the sugar residues, utilising the efficient and selective reaction of aromatic isothiocyanates with 2′-amino groups of oligoribonucleotides (Aurup et al., 1994).

In ribozyme 1, the 2′-amino groups to be crosslinked are within 11 Å in the X-ray structure, but more than 30 Å apart in the FRET model. In contrast, the 2′-amino groups in ribozyme 2 are within 13 Å in the FRET model, but more than 30 Å apart in the X-ray structure. The fully extended crosslink created with reagent **2** spans approximately 16 Å, such that a structure bearing crosslinked residues initially separated by more than 30 Å would be distorted dramatically upon crosslinking. Thus, a hammerhead ribozyme that retained full activity after crosslinking would imply the validity of the corresponding model.

After modification of the 2′-amino groups of ribozymes 1 and 2 with **2** and deprotection of the mercaptan functionalities, the ribozymes were crosslinked by incubation in the presence of oxygen. For both ribozymes, the major product of the crosslinking reaction was isolated and limited alkaline hydrolysis proved that intramolecular crosslinks had been formed between the 2′-amino-modified residues (Fig. 4).

The activities of the crosslinked ribozymes were determined under single-turnover conditions (Fig. 5; Table 1) to monitor the rates of chemical cleavage rather than product release. The crosslinked ribozymes, after reduction, yielded activities similar to that of the original 2′-amino-modified ribozymes, demonstrating that the structures were not perturbed by the chemical modifications per se. However, crosslinked ribozymes differed by some 300-fold: Ribozyme 1 had a cleavage efficiency similar to that of the non-crosslinked species, whereas the activity of ribozyme 2 was reduced dramatically. In fact, the activity of crosslinked ribozyme 2 was accounted for by a contamination of less than 1% of the non-crosslinked material. These results strongly favor the model derived from the X-ray diffraction study as the structure supporting catalysis.

Due to the inherent flexibility of a ribozyme–substrate complex, a kinetically competent conformation cannot be determined unambiguously by measuring the activity of a ribozyme that has been conformationally constrained with a single crosslink. However, the

high catalytic activity of crosslinked hammerhead ribozyme 1 is consistent with a catalytically active conformation with helices I and II in the relative orientation displayed in the X-ray structure. It cannot be rigorously excluded that the inactivity of crosslinked ribozyme 2 might be due to reasons other than distance constraints. This is a potential problem here because the crosslink in ribozyme 2 connects residues that are on the opposite faces of the molecule, which places the crosslink between helices I and II. As a consequence, the crosslink is located close to the nucleotides that comprise the U-turn in the single-stranded region where it might, for example, prevent a conformational change to the transition state or interfere with binding of Mg^{2+}. To rule out the possibility that this particular positioning of the crosslink caused the inactivity of ribozyme 2, we also crosslinked a ribozyme between residues 2.1 and 10.4. The 2′-amino groups of those residues are separated by 13 Å in the FRET model and would place the crosslink on one side of the ribozyme, thus minimizing interactions with the catalytic core. The activity of this ribozyme was similar to that reported for crosslinked ribozyme 2, indicating that the placement of the crosslinks relative to the active site is not critical. Therefore, our results strongly suggest that the relative orientation of helices I and II according to the FRET model cannot be accommodated in an active structure.

Because these results indicate that the current FRET model is incompatible with the catalytically active structure, it raises the question of where this discrepancy originates from. If one assumes that the solution structure of the hammerhead ribozyme is close to that of the crystal structure, the calculated FRET efficiency values for the X-ray structure should agree with the experimental values. Calculated FRET efficiency values based on the orientation of helices in the X-ray structure, with dyes tentatively positioned as previously (Tuschl et al., 1994), are in agreement with the experimental values obtained for the relative orientation of helices I and II with respect to helix III. On the other hand, the high transfer efficiency measured between helices I and II deviates from that calculated for the X-ray structure. However, the FRET methodology has known limitations, namely, uncertainties in the evaluation of κ^2 and in the positioning of the dyes (Tuschl et al., 1994) and it remains to be seen if reevaluation of these parameters will result in calculated transfer efficiencies for the X-ray structure that completely agree with the experimental values.

Our results suggest that FRET analysis may be generally useful for deriving the relative disposition of helices within an RNA molecule. Extension to the next level of detail—a model incorporating the position of every nucleotide—is challenging, especially with a small number of distance constraints and the inherent limitations mentioned above. Thus, the results presented here do not necessarily imply any failure of the FRET technique, but may instead reflect the difficulty of building a high-resolution model from lower-resolution data.

In the absence of X-ray structures of complex, biologically important RNA motifs, one has to rely on other methods for bridging the gap between their secondary and tertiary structures. The methodology described here is, to our knowledge, the first example of site-specific crosslinking through the sugar–phosphate backbone of nucleic acids, and provides a general strategy for extracting information about the tertiary structure of RNAs.

MATERIALS AND METHODS

General

Reactions during synthesis of **2** were carried out under a positive pressure of argon. 2,2′-Dipyridyl disulfide and thiophosgene were purchased from Aldrich. Flash column chromatography was performed on silica gel 60 (Merck) with particle size less than 0.063 mm. HPLC was carried out on a Waters Associates system with a model 6000A pump, a model 680 automated gradient controller, a model 730 data module and a model 481 LC spectrophotometer. Separations were performed on reverse phase material 5 μm ODS Hypersil (Shandon), in a column of dimension 250 × 4 mm. ^{1}H NMR and ^{13}C NMR spectra were recorded in $CDCl_3$ on a Bruker AM 360L instrument at 360.13 and 90.55 MHz, respectively. Chemical shifts are reported in ppm, relative to tetramethylsilane at δ 0.0 ppm. Coupling constants (J) are reported in Hertz. High-resolution, accurate mass spectra (HRMS) were recorded on a on VG analytical Autospec-T tandem mass spectrometer using electron impact ionization.

Oligoribonucleotides were prepared by automated chemical synthesis using phosphoramidites from MilliGen/Biosearch, except for the incorporation of trifluoroacetyl-protected 2′-amino-modified nucleotides (Pieken et al., 1991). Work up of oligoribonucleotides as well as conditions for DPAGE was as described by Tuschl et al. (1993). The 2′-amino-modified ribozymes 1 and 2 were 5′-^{32}P-labeled using T4 polynucleotide kinase and [γ-^{32}P] ATP, and 3′-^{32}P-labeled using T4 RNA ligase and [5′-^{32}P]pCp. Radioactivity in gels was quantified by a Fujix Bio-Imaging Analyzer Bas-2000.

Synthesis of isothiocyanate 3

3-Aminobenzylmercaptan

A solution of 3-aminobenzylalcohol (1.00 g, 8.12 mmol) and thiourea (0.68 g, 8.93 mmol) in 48% aqueous HBr (3.0 mL) was heated at 100 °C for 17 h. To this solution, at 25 °C, was added NaOH (1.42 g, 35.5 mmol) in H_2O (14 mL), followed by heating at 100 °C for 2 h. After cooling to 25 °C, NH_4Cl (1.0 M aq, 60 mL) was added. This mixture was extracted with CH_2Cl_2 (40 mL + 2 × 20 mL), the combined organic phases dried (Na_2SO_4) and the solvent removed in vacuo to give 3-aminobenzylmercaptan (0.38 g, 89%), which was used in the next step without further purification. ^{1}H NMR: δ 2.17

(1H, s, SH), 3.65 (4H, s, NH_2 and CH_2), 6.56 (1H, m, ArH), 6.66 (1H, m, ArH), 6.70 (1H, m, ArH), 7.10 (1H, t, J = 7.7, ArH). ^{13}C NMR: δ 28.8, 113.7, 114.5, 117.9, 129.4, 142.1, 146.7.

2-pyridyl 3-aminobenzyl disulfide (1)

To a solution of 2,2′-dipyridyl disulfide (30.0 g, 136 mmol) and glacial acetic acid (3.2 mL, 55.8 mmol) in ethanol (82 mL) was added dropwise 3-aminobenzylmercaptan (9.46 g, 68.0 mmol) in ethanol (41 mL). After stirring for 2.5 h at 25 °C, the solvent was removed in vacuo and the residue dissolved in CH_2Cl_2 (400 mL) and washed with NaOH (2 M aq, 2 × 200 mL). The combined aqueous phases were extracted with CH_2Cl_2 (200 mL) and the combined organic phases dried (Na_2SO_4) and the solvent removed in vacuo. The product was purified by flash column chromatography (a gradient of 5–50% EtOAc in *n*-hexane) and afforded **1** (10.6 g, 63%) as a pale yellow oil. ^1H NMR: δ 3.70 (2H, bs, NH_2), 3.88 (2H, s, CH_2), 6.48 (1H, m, ArH), 6.56 (1H, m, ArH), 6.64 (1H, m, ArH), 6.99 (2H, m, ArH), 7.51 (2H, m, ArH), 8.39 (1H, m, NCH). ^{13}C NMR: δ 43.8, 114.3, 115.6, 119.1, 119.4, 120.4, 129.4, 136.8, 137.3, 146.8, 149.2, 160.0.

2-pyridyl 3-isothiocyanatobenzyl disulfide (2)

A solution of thiophosgene (4.17 g, 36.3 mmol) in chloroform (50 mL) was treated dropwise with a solution of **1** (8.20 g, 33.0 mmol) in chloroform (250 mL) over 10 min. After stirring for 1 h at 25 °C, the mixture was diluted with CH_2Cl_2 (330 mL) and washed with NaOH (1 M aq, 165 mL). The aqueous phase was extracted with CH_2Cl_2 (40 mL), the combined organic phases dried (Na_2SO_4), and the solvent removed in vacuo. The product was purified by flash column chromatography (CH_2Cl_2), giving **2** (8.80 g, 92%) as a light brown oil. ^1H NMR: δ 3.95 (2H, s, CH_2), 7.01 (2H, m, ArH), 7.12 (1H, m, ArH), 7.18 (2H, m, ArH), 7.44 (1H, m, ArH), 7.51 (1H, m, ArH), 8.41 (1H, m, NCH). ^{13}C NMR: δ 42.7, 119.7, 120.7, 124.6, 126.4, 128.3, 129.5, 131.1, 135.5, 136.7, 138.5, 149.4, 159.2.

Selectivity of thiourea formation at 2′-amino groups in RNA

The oligomers UCGCAUCGCU and UCGCA(2′-NH_2U)CGCU were each incubated with **2** under the conditions described below for ribozymes 1 and 2. After 26 h, aliquots of the reaction mixtures were withdrawn for HPLC analysis. Solvent gradients for analytical HPLC analysis were run at 1 mL/min. Elution was performed with a linear gradient of 50 mM triethylammonium acetate, pH 7.0, containing from 0 to 18% CH_3CN after 15 min, followed by increase to 70% CH_3CN in 5 min, left for 10 min at these conditions, with subsequent return to original conditions (0% CH_3CN) in 3 min. The retention times for the oligomers before the reaction were 10.0 and 9.7 min, respectively. After incubation with the isothiocyanate, the 2′-amino modified oligoribonucleotide was converted (>95%) to a product having a retention time of 15.3 min and the unmodified oligoribonucleotide was unchanged.

Crosslinking of 2′-amino-modified ribozymes

Ribozymes 1 and 2 were each modified using the following procedure. Isothiocyanate **2** was reacted with 5′-^{32}P-labeled ribozyme (50 mM **2**; 1 mM ribozyme; 50 mM borate buffer, pH 8.6; 50% DMF; final volume 10 μL) for 28 h at 37 °C. This reaction mixture was diluted for subsequent annealing of the ribozyme to the noncleavable substrate 5′-GAAUGUdCGG UCGGC (10 μM ribozyme; 20 μM substrate; 50 mM sodium cacodylate, pH 7.5; 50 mM NaCl; final volume 1,270 μL) and the annealing was performed by heating the solution to 90 °C for 3 min followed by slow cooling to 25 °C over a period of 2.5 h. DTT (1 M aq, 127 μL) was added to the solution containing the ribozyme–substrate complex and incubated for 2 h at 25 °C. The oligomers were precipitated at −20 °C after sequential addition of NaOAc (3.0 M aq, pH 5.2; 1,140 μL) and ethanol (9,120 μL), the pellet collected and re-dissolved (10 μM ribozyme; 50 mM sodium cacodylate, pH 7.5; 50 mM NaCl; 20 mM $MgCl_2$; 1,710 μL) The solution was aliquoted into six microfuge tubes and an equal volume of DMSO was added to each. After incubation for 30 h at 25 °C under an atmosphere of oxygen, the RNA was precipitated. The major products of the crosslinking reactions of ribozyme 1 and 2 were purified by 12% and 20% DPAGE, respectively. The crosslinked material was extracted from the gel slices by a crush and soak procedure using NaOAc (1.0 M aq, pH 5.2) from which the products were subsequently precipitated by the addition of ethanol. This resulted in approximately 15% overall yield of crosslinked material.

Limited alkaline hydrolysis

3′-^{32}P-labeled ribozymes 1 and 2 and crosslinked ribozymes 1 and 2 were subjected to limited alkaline hydrolysis (50 mM $NaHCO_3$; final volume 20μL; 100 °C; 5 min), followed by analysis by 20% DPAGE.

Kinetic analysis

Before initiation of kinetics, solutions of ribozyme and substrate RNA (50 mM Tris·HCl, pH 7.5) were preheated separately at 90 °C for 1 min, and cooled to 25 °C over the period of 15 min. This was followed by a further incubation for 15 min at 25 °C in the presence of $MgCl_2$ (10 mM; 50 mM Tris·HCl, pH 7.5). Non-crosslinked ribozymes were obtained by reduction of the crosslinked ribozymes with DTT (5 mM; 50 mM Tris·HCl, pH 7.5) for 4 h at 25 °C prior to heat shock protocol. Trace amount of 5′-^{32}P-labeled substrate (< 1 nM) was incubated in the presence of the ribozymes at varying concentrations (20–300 nM) (50 mM Tris·HCl, pH 7.5; final volume 50 μL; 10 mM $MgCl_2$) at 25 °C, and aliquots (8 μL) withdrawn at appropriate time intervals and added to 16 μL of urea stop mix (3.5 M urea, 25 mM EDTA, 0.02% bromophenol blue, 0.02% xylene cyanol) and subsequently subjected to 20% DPAGE (Tuschl et al., 1993).

ACKNOWLEDGMENTS

We thank T. Heaton and J. Thomson for critical reading of the manuscript. Supported by the Deutsche Forschungsgemeinschaft and the Fonds der Chemischen Industrie. S.Th.S.

gratefully acknowledges a postdoctoral fellowship from the European Molecular Biology Organization.

Received June 12, 1995; returned for revision July 12, 1995; revised manuscript received July 24, 1995

REFERENCES

Amiri KMA, Hagerman PJ. 1994. Global conformation of a self-cleaving hammerhead RNA. *Biochemistry 33*:13172–13177.

Aurup H, Tuschl T, Benseler F, Ludwig J, Eckstein F. 1994. Oligonucleotide duplexes containing 2′-amino-2′-deoxycytidines: Thermal stability and chemical reactivity. *Nucleic Acids Res 22*:20–24.

Bassi GS, Møllegaard NE, Murchie AIH, von Kitzing E, Lilley DMJ. 1995. Ionic interactions and the global conformation of the hammerhead ribozyme. *Nature Struct Biol 2*:45–55.

Beijer B, Sulston I, Sproat B, Rider P, Lamond AI, Neuner P. 1990. Synthesis and applications of oligonucleotides with selected 2′-*O*-methylation using the 2′-*O*-[1-(2-fluorophenyl)-4-methoxypiperidin-4-yl] protecting group. *Nucleic Acids Res 18*:5143–5151.

Bratty J, Chartrand P, Ferbeyre G, Cedergren R. 1993. The hammerhead RNA domain, a model ribozyme. *Biochim Biophys Acta 1216*:345–359.

Butcher SE, Burke JM. 1994. A photo-crosslinkable tertiary structure motif found in functionally distinct RNA molecules is essential for catalytic function of the hairpin ribozyme. *Biochemistry 33*:992–999.

Celander DW, Cech TR. 1991. Visualizing the higher order folding of a catalytic RNA molecule. *Science 251*:401–407.

Dahm SC, Uhlenbeck OC. 1991. Role of divalent metal ions in the hammerhead RNA cleavage reaction. *Biochemistry 30*:9464–9469.

Fedor MJ, Uhlenbeck OC. 1992. Kinetics of intermolecular cleavage by hammerhead ribozymes. *Biochemistry 31*:12042–12054.

Ferentz AE, Verdine GL. 1994. The convertible nucleoside approach: Structural engineering of nucleic acids. *Nucleic Acids Mol Biol. 8*:14–40.

Frank RL, Smith PV. 1946. The preparation of mercaptans from alcohols. *J Am Chem Soc 68*:2103–2104.

Johnson RJ, Chenoweth DE. 1985. Labeling the granulocyte c5a receptor with a unique photoreactive probe. *J Biol Chem 260*:7161–7164.

Krol A, Carbon P. 1989. A guide for probing native small nuclear RNA and ribonucleoprotein structures. *Methods Enzymol 180*:212–227.

Murphy FL, Wang YH, Griffith JD, Cech TR. 1994. Coaxially stacked RNA helices in the catalytic center of the *Tetrahymena* ribozyme. *Science 265*:1709–1712.

Nolan JM, Burke DH, Pace NR. 1993. Circularly permuted tRNAs as specific photoaffinity probes of ribonuclease P RNA structure. *Science 261*:762–765.

Pieken WA, Olsen DB, Benseler F, Aurup H, Eckstein F. 1991. Kinetic characterization of ribonuclease-resistant 2′-modified hammerhead ribozymes. *Science 253*:314–317.

Pley HW, Flaherty KM, McKay DB. 1994. Three-dimensional structure of a hammerhead ribozyme. *Nature 372*:68–74.

Tuschl T, Gohlke C, Jovin TM, Westhof E, Eckstein F. 1994. A three-dimensional model for the hammerhead ribozyme based on fluorescence measurements. *Science 266*:785–788.

Tuschl T, Ng MMP, Pieken W, Benseler F, Eckstein F. 1993. Importance of exocyclic base functional groups of central core guanosines for hammerhead ribozyme activity. *Biochemistry 32*:11658–11668.

Tuschl T, Thomson JB, Eckstein F. 1995. RNA cleavage by small catalytic RNAs. *Curr Opin Struct Biol. 5*:296–302.

Wang JF, Cech TR. 1992. Tertiary structure around the guanosine-binding site of the *Tetrahymena* ribozyme. *Science 256*:526–529.

Wang JF, Downs WD, Cech TR. 1993. Movement of the guide sequence during RNA catalysis by a group I ribozyme. *Science 260*: 504–508.

Woisard A, Favre A, Clivio P, Fourrey JL. 1992. Hammerhead ribozyme tertiary folding: Intrinsic photolabeling studies. *J Am Chem Soc 114*:10072–10074.